

Modelling Mean-Field Games with Neural Ordinary Differential Equations

Anna C.M. Thöni

Department of Artificial Intelligence
Radboud University
Nijmegen, the Netherlands
chiara.thoeni@ru.nl

Yoram Bachrach

Meta
London, United Kingdom
yorambac@meta.com

Tal Kachman

Department of Artificial Intelligence
Radboud University
Nijmegen, the Netherlands
tal.kachman@ru.nl

Abstract

Mean-field game theory relies on approximating games that would otherwise have been intractable to model. While the games can be solved analytically via the associated system of partial derivatives, this approach is not model-free, can lead to the loss of the existence or uniqueness of solutions and may suffer from modelling bias. To reduce the dependency between the model and the game, we combine mean-field game theory with deep learning in the form of neural ordinary differential equations. The resulting model is data-driven, lightweight and can learn extensive strategic interactions that are hard to capture using mean-field theory alone. In addition, the model is based on automatic differentiation, making it more robust and objective than approaches based on finite differences. We highlight the efficiency and flexibility of our approach by solving three mean-field games that vary in their complexity, observability and the presence of noise. Using these results, we show that the model is flexible, lightweight and requires few observations to learn the distribution underlying the data.

1 Introduction

Game theory investigates strategic interactions between self-interested agents that inhabit the same environment and are affected by each other's actions. Such analysis has applications in economics [1–3], crowd motions [4, 5] and evolutionary biology [6]. We propose neural network-based methods to solve mean-field games (MFGs), which describe games with an extremely large (or, in the limit, infinite) population of agents [7, 8]. MFG theory has been introduced by Lasry and Lions [8] and Huang et al. [7] and borrows methodologies from particle physics. Given the large number of particles in this field, it is expensive at best and intractable at worst to model all inter-particle interactions. Instead, mean-field theory replaces the particles with their mean-field, the distribution from which

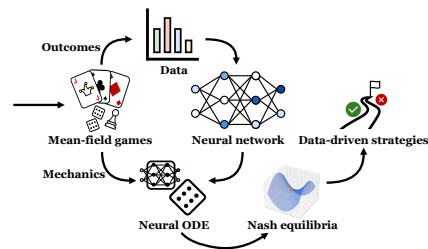


Figure 1: An overview of modelling MFGs with neural ODEs. The neural ODE combines the MFG mechanics with the neural network output to create more informed strategies.

Table 1: An overview of the mean-field games included in the Experiments.

Game	Observability	Neural network input	Neural network output
Meeting arrival times	Full	Observed arrival times	Intended arrival times
El Farol Bar problem	Full	Observed attendance rates	Probability of going to the bar
Liars dice	Partial	Dice outcomes, dice odds and bluff strategy	Dice odds and bluff strategy

the theory derives its name [9]. From a mathematical perspective, this distribution is described with two coupled differential equations: the Hamilton-Jacobi equation for expressing the change in dynamics of a single particle; and the Fokker-Planck equation that describes the mean-field density summarizing the interactions between all other particles [8, 10].

When games are considered, the atomic agents of interest become more complex: in contrast to fundamental particles, players can perceive and act on their environment, which allows for strategic decision-making. To accommodate this rationality, while still being able to construct a mean-field, MFG theory relies on assumptions of symmetry and homogeneity [8].

The analysis of MFGs concerns optimality conditions that arise from the joint minimization of the agents’ costs. The optimal control leading to such a minimum is found by solving the partial or stochastic differential equations (DEs) accompanying the MFG [10]. These systems can be solved numerically by discretizing the differential equations using finite differences [11, 12]. However, solving a system of differential equations involving high-dimensional agent states is challenged by the curse of dimensionality [13, 14]. In addition, the discretization introduces an error that is subject to the chosen method and may ultimately lead to the loss of the existence or uniqueness of the solutions [15].

Instead, the solutions to the mean-field game can be approximated using artificial neural networks [16], in the form of recurrent architectures [17, 18], deep policy iteration [19], deep Galerkin methods [20] or actor-critic-based approaches [21, 15, 22]. Still, all approaches mentioned above are DE-based and require full knowledge of the game of interest. This dependency limits the models’ applications and may introduce a modelling bias. Reinforcement learning (RL)-based solutions surmount this requirement by building upon the Fictitious Play algorithm instead of following a numerically exact approach [23–27]. Because the Fictitious Play algorithm is independent of the modelled system, the RL-based algorithms are commonly referred to as “model-free” [13].

To retain the numerical exactness of the DE-based solutions without requiring full knowledge of the game of interest, we propose to analyze MFGs using neural ordinary differential equations (neural ODEs; Chen et al., 2018). To do so, we complement the existing system of DEs with a neural network (Figure 1). The resulting model is data-driven and may therefore alleviate modelling bias associated with the predefined MFG dynamics. Furthermore, the model’s ability to recover structure from data allows it to reason beyond the predefined DEs. Lastly, the neural ODEs are solved using automatic differentiation, which makes them more robust than the DE-based solutions based on discretization [29]. This property is, in combination with the model’s data-driven nature, expected to prevent the loss of the existence of solutions that affect the original PDE-based approaches.

Contributions To the best of our knowledge, we are the first to combine mean-field mechanics with deep learning in this way. Therefore, the contributions of this paper are threefold: (1) We provide the theoretical framework for combining MFG theory with neural ODEs, (2) we reformulate examples from classical game theory to their MFG counterparts, taking the continuum limit on the number of agents by leveraging the structure of the neural ODEs, and (3) we test the neural ODEs on the games presented in Table 1 to give a proof of concept of the model’s ability to construct new (data-driven) Nash equilibria by empirically highlighting emerging strategies.

2 Background

We combine the concepts of mean-field games with neural ODEs. We use bold characters to denote vectors.

2.1 Mean-Field Games

Depending on the context, the MFGs are commonly described using partial differential equations (PDEs) or concepts from reinforcement learning. This section considers the PDE perspective, making it easier to unite the MFGs with the neural ODEs discussed later.

To introduce the system of PDEs describing the game, consider a system of N agents. Each agent $i \in [1, \dots, N]$ has a state at time $t \in [t_0, T]$, denoted with $\mathbf{x}_t^i \in \mathbb{R}^d$. The state of agent i evolves over time according to their control, or game-playing strategy, α_t^i . The dynamics of a single agent can be described according to the Itô process presented in Equation 1, combining their drift function b with a diffusion driven by a Brownian motion. The strategies of all other agents are accounted for with the inclusion of m , a probability measure representing the mean-field [25]. ν is a nonnegative parameter.

$$\frac{d\mathbf{x}}{dt} = b(\mathbf{x}_t^i, \alpha_t^i, m(t)) + \sqrt{2\nu}B_t \quad (1)$$

The agents' state evolves by the repeated application of their drift and diffusion, such that $\mathbf{x}_{t+1} = \mathbf{x}_t + b(\mathbf{x}_t^i, \alpha_t^i, m(t)) + \sqrt{2\nu}B_t$. Having the freedom to optimize their control in \mathbb{R}^k , the agents minimize the cost function J .

$$J^i = \mathbb{E} \left[\int_{t_0}^T \frac{1}{2} L(\mathbf{x}_s^i, m(s), \alpha_s^i) ds + G(\mathbf{x}_T^i, m(T)) \right] \quad (2)$$

Following the fundamentals of dynamic programming, J combines the evolution of the agents' cost L through s with a terminal cost G at the state T . Just like the agents' dynamics, the cost function links the agents' individual states x to the mean-field m . Assuming that agent i is a representative agent in the system, it is implied that all agents aim to minimize the cost function. Therefore, it is natural to analyze the MFG with the generalized notion of the *Nash equilibrium*, which is reached for a family of controls ($\bar{\alpha}$) when it holds that

$$\forall i, j \in [1, \dots, N], J^i(\bar{\alpha}^i, \bar{\alpha}_{j \neq i}^j) \leq J^i(\alpha^i, \bar{\alpha}_{j \neq i}^j) \quad (3)$$

for all non-Nash strategies α^i [30]. That is, the Nash equilibrium is a fixed point in the space of the flow in m [31], which implies that no agent benefits from changing their strategy if a Nash equilibrium is reached. Computing the Nash equilibria for many agents involves a large set of controls and can be a lot of work. Fortunately, the symmetry assumption of the theory simplifies this problem, facilitating the calculation of Nash equilibria when $N \rightarrow \infty$. We refer the reader to Cardaliaguet [10] for a detailed account of this simplification. MFGs have been formalized by Lasry and Lions [8] as a system of PDEs (Equation 4), consisting of (a) a Hamilton-Jacobi-Bellman (HJB) equation providing the necessary and sufficient conditions for the optimality of α w.r.t. J and (b) a Fokker-Plank (FP) equation describing the evolution of the mean-field according to the dynamics presented in Equation 1. Their Nash equilibria are associated with the local minima of the cost J , which can be found by solving Equation 4.

$$\begin{cases} \text{(a)} & -\partial_t u - \nu \Delta u + H(\mathbf{x}, m, Du) = 0 & \text{in } \mathbb{R}^d \times (0, T) \\ \text{(b)} & \partial_t m - \nu \Delta m - \text{div}(D_p H(\mathbf{x}, m, Du) m) = 0 & \text{in } \mathbb{R}^d \times (0, T) \\ \text{(c)} & m(0) = m_0, u(\mathbf{x}, T) = G(\mathbf{x}, m(T)) \end{cases} \quad (4)$$

The coupling of the HJB and FP equations is facilitated via the unknowns u and m . In particular, the first equation goes backwards in time and describes the value function of a single agent, u . The second goes forward in time and describes the change in the mean-field density m . The equation is parameterized with the nonlinear function H , which is the Fenchel conjugate to L w.r.t. the mean-field probability p . In addition, D is used to denote a differential operator. Both equations are subject to two structure conditions. Firstly, $H(\mathbf{x}, m, p)$ is convex with respect to p . This is required to satisfy the optimality condition provided by the HJB equation. Secondly, m is a probability measure with the initial state m_0 (Equation 4c). In addition to the structure conditions, the terminal condition $u(\mathbf{x}, T) = G(\mathbf{x}, m(T))$ relates Equation 4 back to the cost presented in Equation 2 [8, 10].

2.2 Neural Ordinary Differential Equations

Neural ODEs are a neural network-based method introduced by Chen et al. [28]. To illustrate the method, we return to the SDE introduced in Equation 1 and call it h . To learn the development of the agent’s dynamics over time, we can solve the initial value problem (IVP) consisting of the agent’s initial state $\mathbf{x}(t_0) = \mathbf{x}_0$ and the ODE describing their dynamics $\frac{d\mathbf{x}}{dt} = h(t, \mathbf{x}(t))$. The solution to this problem is commonly calculated using discretization, transforming the continuous function h into a counterpart that consists of small steps [32]. $\mathbf{x}(t)$ is updated step-by-step by adding its identity to $h(t, \mathbf{x}(t))$, the output of the ODE. This process is illustrated in Equation 5, where Δt denotes the discretized stepsize.

$$\mathbf{x}(t + \Delta t) = \mathbf{x}(t) + h(t, \mathbf{x}(t)) \quad (5)$$

Chen et al. [28] highlight the similarity between the discretization of continuous functions and the residual motif $y = F(\mathbf{x}) + \mathbf{x}$ from ResNet architectures [33]. They compare the addition of the identity $\mathbf{x}(t)$ to the residual skip connections, relating the discretization steps to the repeated application of the residual blocks F . This analogy lays the foundation for neural ODEs: a class of differential equations expressed as a neural network. Thus, instead of discretizing a concrete mathematical function h , the neural ODE repeatedly applies the data-driven output of a neural network f . The discretized step size, Δt is optimized by the ODE solver and may vary throughout the solving process. As a consequence, a neural ODE can be seen as a neural network with a flexible, and in the limit, infinite, number of layers. The output of the solver can be regarded as a latent trajectory over time, where each output z_{t_0}, \dots, z_T represents the latent state [28]. Because the neural ODEs are trained using reverse automatic differentiation and the adjoint sensitivity method [34], the user has explicit control of the model’s numerical error [28].

Neural ODEs are fully data-driven because they are solely specified in terms of a neural network f . All the while, dynamical systems may be described using domain knowledge based on scientific models or physical laws. Rackauckas et al. [35] unify the above with the introduction of universal differential equations (UDEs), combining the output of f with that of a concrete ODE h : $\frac{d\mathbf{x}}{dt} = h(t, \mathbf{x}(t)) + f(\mathbf{x})$. In this case, f can be trained to yield insights that go beyond the predefined ODE h . A stochastic UDE variant has already been used to solve a HJB equation, highlighting the model’s adaptivity, efficiency and flexibility towards stiffness [35].

3 Methods

In this work, we introduce a new perspective on UDEs by combining existing MFG specifications with neural ODEs.¹ We include the neural ODE at the agent level. This way, the neural network output may provide additional insights drawn from the mean-field, past game states or observations (see Table 1). Because these insights directly inform the agents’ value function u , the agents are expected to make better-informed decisions. In addition, this approach leverages the setup of the neural ODE, which allows for taking the number of agents or turns to the continuum limit. Our approach updates the MFG specification presented in Section 2.1. In particular, we extend the HJB equation from Equation 4a according to Section 2.2, such that

$$-\partial_t u - \nu \Delta u + H(\mathbf{x}, m, Du) + f(t, \mathbf{x}, m, Du) = 0 \quad (6)$$

The rest of Equation 4 remains unchanged, albeit the new HJB indirectly affects the evolution of m described in Equation 4b. Even though it might be tempting to supply each agent with their own network to increase the diversity of strategies, this approach drastically reduces the scalability of the method. Thus, we use a single neural network per MFG. More specifically, we use a multilayer perceptron with 3 hidden layers of 8 neurons. Even though the network seems very small, we stress that it’s applied repeatedly during the ODE solve, which increases its capacity. The network uses Softplus activations and is optimized with Adabelief [36]. The learning rate is 5×10^{-4} . The experimental framework has been implemented in Python. We use Optax, Diffrax and Equinox to connect the methods to the JAX ecosystem [37–39].

¹Despite being coined as UDEs by Rackauckas et al. [35], we continue using the term “neural ODE” for our model. This is because the latter term is prevalent in the literature.

4 Experiments

We demonstrate the capacity and flexibility of the neural ODEs by solving three example games. We start with the *meeting arrival times* game [9], a toy example considering a distribution of (unbounded) arrival times. With the *El Farol Bar problem* [40], we discuss a more complex game that requires the estimation of probabilities. Lastly, we consider *Liar’s dice*, a game including probabilities, imperfect-information and deceit. All experiments have been performed on an Apple M1 Pro CPU with 16 GB RAM.

4.1 Meeting Arrival Times

The *meeting arrival times* game, introduced by Guéant et al. [9, p. 9], illustrates a simple MFG application. The game considers a meeting that is scheduled at time s . Despite this planning, the true starting time of the meeting \tilde{s} depends on the fraction of agents that have arrived. It holds that $\tilde{s} \geq s$, meaning that the meeting starts later if the quorum has not been reached at time s . Each agent i has an intended arrival time τ^i and actual arrival time $\tilde{\tau}^i$. The agents control τ , but $\tilde{\tau}^i$ is subject to the uncertainty $\tilde{\epsilon}^i$ such that $\tilde{\tau}^i = \tau^i + \tilde{\epsilon}^i$. In our implementation of the game, $\tilde{\epsilon}^i$ is drawn from the Gaussian $\mathcal{N}(0, 1)$.

To build upon the formalism introduced in Section 2.1, consider that the agents optimize their intended arrival time by minimizing the cost J . For this game, J is the sum of the components $j_{[1-3]}$, presented below. The notation $[\cdot]_+$ is shorthand for $\max(\cdot, 0)$.

- j_1 **The reputation effect** A cost associated with the lateness to the originally scheduled time s . $j_1(s, \tilde{\tau}) = [\tilde{\tau} - s, 0]_+$
- j_2 **A personal inconvenience** A cost associated with the lateness to the actual starting time \tilde{s} . $j_2(\tilde{s}, \tilde{\tau}) = [\tilde{\tau} - \tilde{s}, 0]_+$
- j_3 **The waiting time** A cost associated with arriving earlier than the actual starting time \tilde{s} . $j_3(\tilde{s}, \tilde{\tau}) = [\tilde{s} - \tilde{\tau}, 0]_+$

The behaviour of all other agents is summarized in the actual starting time \tilde{s} , which is the mean-field of this game by summarizing all the agents’ actions in a cumulative distribution of arrival times. To acknowledge the coupling between \tilde{s} and the individual agents, consider that each agent bases their intended arrival τ^i time on \tilde{s} and \tilde{s} is influenced by the cumulative distribution of all actual arrival times $\tilde{\tau}^i$. In addition, Guéant et al. prove that \tilde{s} exists, being a unique fixed point representing the game’s equilibrium.

We model the “standard” version of the game with a SDE that differentiates over the turns t (see Equation 1). Even though the game lacks a terminal condition, we treat it as a finite game by setting $t \in [1, 15]$. Figure 2a shows an example outcome of the game, where the distribution of arrival times quickly narrows down. This observation is in accord with the proof provided by Guéant et al. The exact value of \tilde{s} diffuses between turns due to the Brownian motion in the SDE. While the original game description does not include Brownian motion, it is included in this example to demonstrate the modelling capacity of the neural ODE.

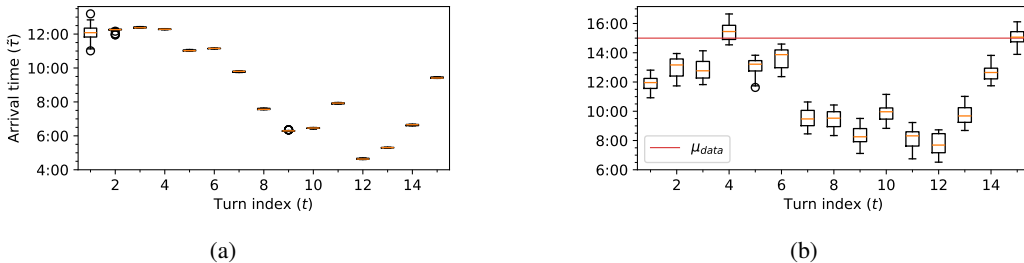


Figure 2: The distribution of meeting arrival times for the standard (a) and the neural ODE (b) version of the *meeting arrival times* game. In (a), the randomly initialized distribution of arrival times quickly converges to a narrow distribution centred at \tilde{s} . The value of \tilde{s} is subject to the Brownian noise of the SDE. In (b), the distribution of *meeting arrival times* of agents whose control is steered towards arriving at 15:00 in turn 15.

4.1.1 Learning the intended arrival times

To apply the neural ODE, we create a data-driven challenge and aim to find the meeting time s that aligns with a collection of observed arrival times. To this end, we convert the SDE into a neural ODE by adding the output of a feedforward neural network f . f is trained to minimize the difference between the modelled arrival times at turn 15 and the “true” observed arrival times, $\tilde{\tau}^*$. We train on 10 games. For each game, $\tilde{\tau}^*$ is generated by drawing M samples from N different Gaussians $\mathcal{N}(\mu_i, \sigma_i)$ for $i \in [1, 2, \dots, N]$. Each μ_i is sampled from $\mathcal{N}(15, 0.5)$, while $\sigma_i \sim \Gamma(2, 0.2)$. As a result $\tilde{\tau}^*$ consists of $N \times M$ observations that form a noisy reflection of the distribution of intended arrival times around 15:00. The neural ODE models the interplay between the game rules and the observed data by minimizing the neural network loss alongside the agents’ cost J . The results are shown in Figure 2b. The initial random distribution is centred around 12:00. Despite the small network size and the Brownian motion, the neural ODE can converge around $s = 15:00$ in turn 15.

4.2 The El Farol Bar Problem

Even though the meeting time arrival game provides a proof of concept, the neural ODE does not yield additional insights into the game dynamics. Therefore, we consider an implementation of the *El Farol Bar problem*, a more complex example introduced by Arthur [40]. In this problem, a fixed population of agents can go to a bar. Each agent i goes to the bar with a probability p_i , and all agents need to decide simultaneously whether they’re going. The agents’ utility depends on the bar’s crowdedness. If the bar is too crowded, all the agents that went there regret their decision and have less fun than the ones that stayed at home.

The cost function J associated with the bar problem is comparable to that of the *meeting arrival times* game. However, the new cost function is selective; not all components apply to all agents. This selectivity is presumed to lead to an interplay between the MFG dynamics and the neural network. The cost is parameterized by the agent’s probability of going to the bar (p), the fraction of agents that went to the bar (a), and the crowding threshold (c). J consists of the sum of $j_{[1-3]}$ described below.

j_1 **Missed a good evening** The cost associated with staying at home while the bar was not too crowded. This cost only applies to agents that did not go to the bar.

$$j_1(p, a, c) = \begin{cases} 0 & \text{if } a \geq c \\ [c - p]_+ & \text{if } a < c \end{cases}$$

j_2 **Crowding penalty** The cost associated with going to a full bar. This cost only applies to the agents that went to the bar.

$$j_2(p, a, c) = \begin{cases} [p - c]_+ & \text{if } a \geq c \\ 0 & \text{if } a < c \end{cases}$$

j_3 **Peer pressure** The cost inflicted due to not conforming with the rest of the agents. This cost does not depend on C and applies to all agents.

$$j_3(p, a) = (p - a)^2$$

In contrast with the *meeting arrival times* game, the value function of the *El Farol Bar problem* does not include a Brownian motion. Instead, it is modelled as an ODE differentiating over $t \in [1, 15]$, where each turn presents a new opportunity to go to the bar. As the distribution of agents is summarized in the fraction of agents that went to the bar, a can be considered the mean-field of the game. The agents reach a Nash equilibrium when the mean probability of going to the bar converges to the crowding threshold [40]. This behaviour is highlighted in Figure 3a. The figure shows the evolution of the distribution of agents, where p goes from a uniform distribution on the interval $[0.0, 0.1]$ at turn 1, to a narrow distribution centred around $c = 0.9$ at turn 15.

4.2.1 Observed attendance rates and emerging strategies

Whereas the dynamics observed in Figure 3a purely emerge from the game’s setup, we test whether a combination of the game rules with observed attendance rates leads to more informed strategies. To generate observations, we consider $N \times M$ agents. To create a single data point $\mathbf{x} \in \mathbb{R}^{10}$, the agents’ attendance rates are monitored for 10 subsequent turns. The attendance rate of one evening is generated by summing over $j \in [1, 2, \dots, N \times M]$ samples drawn from *Bern*(p_j). Just like the arrival times data, the vector of probabilities is created by drawing M samples from N different Gaussians $\mathcal{N}(\mu_i, \sigma_i)$ for $i \in [1, 2, \dots, N]$. The hyperparameters are the same for both games. However, the agents’ intentions p_j are limited to the domain $[0, 1]$ to represent a probability.

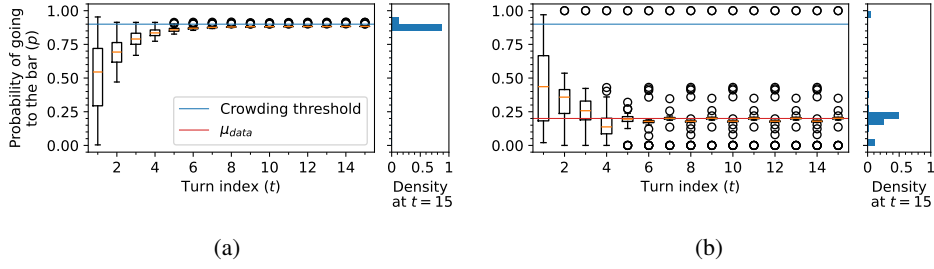


Figure 3: The distribution of probabilities of going to the bar for the standard (a) and neural ODE (b) version of the *El Farol Bar problem*. In the standard version, the distribution of probabilities converges towards the crowding threshold of $c = 0.9$ (blue). The neural ODE (b) is trained to align with the observed attendance rates, where the mean is indicated in red. The density histograms show the normalized distributions at turn 15.

To discover how the agents' probabilities of going to the bar change after training on 10 observations in \mathbb{R}^{10} , we deliberately diverge from the MFG setup by distributing the observed attendance rates around $\mu_0 = 0.2$ (Figure 3b, red). Note that μ_0 is significantly below the crowding threshold $c = 0.9$ (Figure 3b, blue). Even though the agents can only decide on a single output value, the neural ODE allows the agents to build more complex strategies than the standard MFG. Namely, the MFG-based agents in Figure 3a converge to an almost homogeneous strategy $p = c$. In contrast, the results from Figure 3b are more widely distributed. Furthermore, the distribution "oscillates" between turns. This oscillation results from the interplay between j_1 , drawing the agents towards the crowding threshold, and the combination of the neural network contribution and j_3 , pulling the agents back to μ_0 . Regardless of the oscillations, there are a few agents with $p = 1.0$, always going to the bar, independent of the other strategies. The agents from the last category leverage the fact that the majority of agents have a low probability of going to the bar. Because of this, they can always go to a bar that is never too crowded.

4.3 Liar's Dice

The last game discussed is *Liar's dice*, a dice game that starts with M players rolling D dice with N faces each. Next, the players take turns, estimating the number of occurrences of a specific face in all dice rolls. The first player makes an opening bid, e.g. stating that there are 2 dice with face 4. Every subsequent player may bid a higher quantity of dice with the same face; a higher quantity of dice with a higher face; or the same quantity of dice with a higher face. Alternatively, a player may challenge the previous bid, ending the round. If the combined number of dice is smaller than the bidding quantity, the challenge is successful and the challenging player wins the round. The challenge is unsuccessful if the combined number of dice is larger than or equal to the bidding quantity, in which case the player who made the last bid wins.

In this partially observable game, the players aim to make deceitful, but probable bids. Therefore, the players' utility is based on (1) their ability to bluff and (2) the correctness of their estimate of the dice odds. As it is very hard to capture these ideas in an appropriate cost function, we model J as a starting point. We deliberately leave room for the neural network to learn the missing details leading to the optimal control. In short, J is the sum of $j_1(q_t, q_{t-1}, m_q) = [m_q - (q_t - q_{t-1})]_+$, $j_2(q_t, a) = [a - q_t]_+$ and $j_3(f_t, m_f) = [m_f - f_t]_+$, explained below.

- j_1 **Safety penalty** A penalty for being on the safe side when increasing the bid's quantity, making it easier for the next player to make a plausible bid. A metric of the quantities of the current (q_t) and previous (q_{t-1}) bid, and the maximal possible quantity of the face of interest (m_q).
- j_2 **Bluffing risk** A penalty for bluffing too much, making the bids improbable and increasing the risk of losing a challenge. A metric of the quantity of the current bid (q_c) and the actual number of times the face of interest is thrown (a).
- j_3 **Niceness penalty** A penalty for not increasing the face of the bids, leaving more room for the other players to make a plausible bid. A metric of the largest face of the die m_f and the face associated with the current bid f_t .

Just like the games discussed previously, *Liar’s dice* is solved by differentiating over the turns t . Interestingly, the continuity of the turns z_{t_0}, \dots, z_T makes the setup *non-atomic*: each turn represents the actions of a single player, translating the continuum of turns z into a continuum of players [41]. This contrasts with a discrete, turn-based game where the number of turns, and thus players, is fixed.

Because the players do not share the outcome of their dice throws, their bidding strategy depends on their own (noiseless) outcome and the (noisy) beliefs about all other throws. To make this problem more complex, the dice are not guaranteed to be fair. Therefore, the mean-field summarizes all players $i \in [1, \dots, N]$ by their beliefs $\hat{\theta}_t^i$ parameterizing the categorical distribution describing the dice throws. In addition, the players have a likelihood of making deceitful bids. The bluffing mechanism is implemented with a Poisson distribution that is characterized by the λ_t^i , a learnable bluff parameter. The players can optimize their bluffing strategy and beliefs about the dice distribution by minimizing their cost. However, there is no easy analytical formulation for the problem presented here, as the cost is underdefined. This makes it hard to find an analytical solution for its Nash equilibrium. Instead, we make an approximation by combining the ODE describing the MFG with a neural ODE. We train the model on 1000 rounds of the *Liar’s dice* game, creating a setup that is comparable to the iterated prisoner’s dilemma. We train on a relatively large number of rounds to stabilize the analyses of the bluffing strategy that has a lot of local minima.

In each round, we draw D dice throws from a categorical distribution parameterized by the true dice odds θ . Next, the player’s bid is based on the MFG drift and the neural network output. The interested reader will find the pseudocode for the drift in Appendix A. The neural network output differs per turn t and depends on $\hat{\theta}_t^i$ of the current player, the current player’s dice outcomes and the previous player’s bid. The neural network parameters are only updated when the round has ended. The loss fuelling this update consists of the mean squared error between the $\hat{\theta}_t^i$ and the distribution estimated from all dice outcomes revealed at the end of the round. In addition, the loss includes a term based on the correctness of the challenge. This term adds the batch-wise ratio of correct challenges to the loss, penalizing the network if a game ends with a correct challenge and optimizing λ .

4.3.1 Informed Bluffing

As *Liar’s dice* does not have a clear Nash equilibrium, we compare the strategies that emerge from the MFG mechanics and the neural ODE. More specifically, we analyze the agents’ bluffing strategies λ_t^i . We play the game with $N = 30$ players that have $D = 15$ dice each. The players’ strategies are valued in terms of the learned bluff strategy and the length of the games played. To isolate the bluffing effect, we assume that the dice are fair and the players’ beliefs about the dice are correct, i.e. $\hat{\theta}_0 = \theta$.

Figure 4a shows the influence of the initial bluff strategy on the game length. The results from Figure 4a suggest that the strategy from the neural ODE players (orange) tends to yield shorter games for $\lambda_0 < 3$ compared to the strategy based on the MFG dynamics (blue). This effect is caused by the larger drift of λ in the neural ODE, where the neural ODE-based players are more likely to learn larger values for λ_t for $t > 0$ when λ_0 is small (Figure 4b). Despite the more risky bluffing strategy of the neural ODE strategy, there is no strong evidence of an increase in the number of successful challenges. The relation between the bluffing strategies and the ratio of successful challenges is further explored in Appendix B.

4.3.2 Estimating the Dice Odds

We test the efficiency of the model by testing its resilience against an incorrect belief $\hat{\theta}_0$. To do so, we simulate a new series of games, where $N = 2$ agents unknowingly play with $D = 2$ (the same) unfair dice, i.e. $\hat{\theta}_0 \neq \theta$. The agents can only update their beliefs when a game ends and all four dice are revealed to verify the challenge. Given the loss function, it is expected that the more dice the agents see, the likelier they are to update their beliefs. This behaviour is summarized in Figure 5, which relates the Kullback-Leibler divergence between the true and estimated dice odds to the number of dice seen during training.² Even though the model is not solving a difficult task, it is still very effective and converges after seeing around 15 dice.

²Because the KL divergences are so small, we ignore the loss component regarding the bluff parameter for clarity.

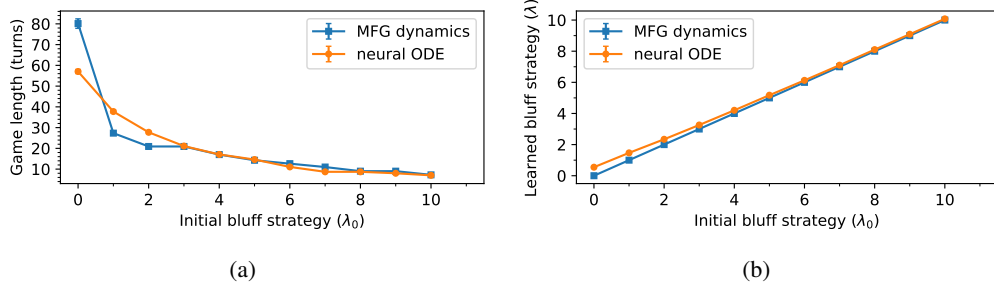


Figure 4: Dice game analyses. Left: the average game length as a function of the initial bluff strategy λ_0 . Right: relation between the initial bluff parameter λ_0 and the average bluff parameter that has been learned throughout the game. Both figures present an average that is aggregated over 100 games. The error bars indicate a standard deviation from this average.

5 Discussion

Neural ODEs form a powerful tool for influencing the Nash equilibria of a game. Our experimental results highlight the model’s strengths: the results found with *meeting arrival times* game underline its ability to learn abstractions from data, even under noisy circumstances. In addition, the analyses of the *El Farol bar problem* exemplify strategies that emerge from the interaction between the data-driven dynamics and the MFG mechanics. Lastly, the neural ODE can learn more elaborate strategies without training on external observations. When training the neural ODE in the context of *Liar’s dice*, we obtain new bluffing strategies when applying the neural network to observations made in previous game states.

Limitations A limitation of our methods is that the neural network introduces a “black box” into the game dynamics. In particular, the inclusion of the neural network reduces the game’s general interpretability by making the agents’ decisions more opaque. Furthermore, the formulation of the model is limited by the symmetry assumption of the MFG. Because of the large number of players involved, the neural network has to be shared between agents. While this does not imply that the agents have identical beliefs, they are still linked through the neural network parameters.

6 Conclusion

Mean-field game theory is used to efficiently model games with a very large to infinite population of agents. The agents’ Nash equilibria are commonly found via reinforcement learning or by solving the system of PDEs associated with the MFG. Both methods have their advantages, the first being model-free and the second numerically exact. To get the best of both worlds, we extend the PDE formulation of the MFG with a neural network. The resulting neural ODE exerts a data-driven influence on the game’s Nash equilibria, deriving strategies that are in line with observed game outcomes. In addition, it can be trained to recover structure from the game’s past dynamics, learning more complex strategies without using extra data. Leveraging those properties, the model can fill in dynamics that are unaccounted for in the original MFG specification. Thus, the addition of the neural network not only makes it easier to model MFGs, but also decreases the modelling bias compared to fully specified systems of PDEs. Besides their ability to incorporate observations, neural ODEs are a numerically exact and lightweight alternative to (deep) RL-based methods for solving MFGs. To match the RL-based methods in their flexibility, the neural ODE can be made completely model-free by fully omitting the predefined partial derivatives. Lastly, their dependency on automatic

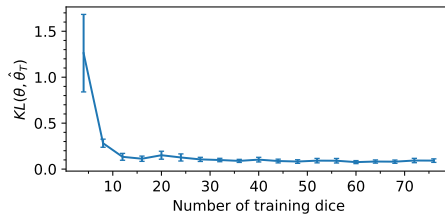


Figure 5: The KL divergence between the true (θ) and estimated ($\hat{\theta}_T$) dice odds as a function of the number of training dice considered. The KL divergence was averaged for all players in 100 games. The error bars indicate a standard deviation from this average.

differentiation makes the neural ODEs more objective than approaches that solve PDEs using finite differences [28, 29], which may prevent the loss of existence or uniqueness of solutions associated with solving MFGs [15].

Even though we only consider simple, synthetic games, we hope that our work provides sufficient proof of concept to inspire future research on data-driven modelling of MFGs. For example, neural ODEs could be used to formulate poker, as has been done with deep counterfactual regret minimization by Brown [42]. Alternatively, the neural ODEs can be elaborated on by using a fixed number of neural networks to model subpopulations of agents. Such models could find applications in settings used to analyse collaborative or adversarial strategies. In addition to solving more complex games, we expect the model to find applications in systems associated with non-atomic, anonymous players and observations, which are commonly found in markets and economics [43].

Software and Data

The source code associated with the methods and experiments is available on GitHub: <https://github.com/KachmanLab/MFGSandbox>. All software was prepared by the Radboud University authors.

References

- [1] Robert Gibbons. *Game Theory for Applied Economists*. Princeton University Press, 1992. ISBN 9780691003955.
- [2] David Easley, Jon Kleinberg, et al. *Networks, crowds, and markets: Reasoning about a highly connected world*, volume 1. Cambridge university press Cambridge, 2010. doi:10.1017/CBO9780511761942.
- [3] Yves Achdou, Jiequn Han, Jean-Michel Lasry, Pierre-Louis Lions, and Benjamin Moll. Income and Wealth Distribution in Macroeconomics: A Continuous-Time Approach. *The Review of Economic Studies*, 89(1):45–86, 04 2021. ISSN 0034-6527. doi:10.1093/restud/rdab002.
- [4] Yves Achdou, Pierre Cardaliaguet, François Delarue, Alessio Porretta, and Filippo Santambrogio. *Mean Field Games*, volume 2281. Springer, 2019. doi:10.1007/978-3-030-59837-2.
- [5] Alexander Aurell and Boualem Djehiche. Modeling tagged pedestrian motion: A mean-field type game approach. *Transportation Research Part B: Methodological*, 121:168–183, 2019. ISSN 0191-2615. doi:10.1016/j.trb.2019.01.011.
- [6] J. McKenzie Alexander. Evolutionary Game Theory. In Edward N. Zalta, editor, *The Stanford Encyclopedia of Philosophy*. Metaphysics Research Lab, Stanford University, Summer 2021 edition, 2021. doi:10.1017/9781108582063.
- [7] Minyi Huang, Roland P. Malhamé, and Peter E. Caines. Large population stochastic dynamic games: closed-loop McKean-Vlasov systems and the Nash certainty equivalence principle. *Communications in Information & Systems*, 6(3):221 – 252, 2006. doi:10.4310/CIS.2006.v6.n3.a5.
- [8] Jean-Michel Lasry and Pierre-Louis Lions. Mean Field Games. *Japanese Journal of Mathematics*, 2:229–260, 03 2007. doi:10.1007/s11537-007-0657-8.
- [9] Olivier Guéant, Jean-Michel Lasry, and Pierre-Louis Lions. *Mean Field Games and Applications*, pages 205–266. Springer Berlin Heidelberg, Berlin, Heidelberg, 2011. ISBN 978-3-642-14660-2. doi:10.1007/978-3-642-14660-2_3.
- [10] Pierre Cardaliaguet. Notes on Mean Field Games, 09 2013.
- [11] Luis Briceño-Arias, Dante Kalise, Ziad Kobeissi, Mathieu Laurière, Álvaro Mateos González, and Francisco Silva. On the implementation of a primal-dual algorithm for second order time-dependent Mean Field Games with local couplings. *ESAIM: Proceedings and Surveys*, 65: 330–348, 01 2019. doi:10.1051/proc/201965330.

- [12] Yves Achdou and Italo Capuzzo-Dolcetta. Mean field games: Numerical methods. *SIAM Journal on Numerical Analysis*, 48(3):1136–1162, 2010. doi:10.1137/090758477.
- [13] Mathieu Laurière, Sarah Perrin, Matthieu Geist, and Olivier Pietquin. Learning Mean Field Games: A Survey. *arXiv*, 05 2022. doi:10.48550/arXiv.2205.12944.
- [14] Richard Bellman. A Markovian decision process. *Journal of mathematics and mechanics*, pages 679–684, 1957. doi:10.1512/IUMJ.1957.6.56038.
- [15] Zejian Zhou, Yuzhu Zhang, and Hao Xu. Reinforcement Learning-based Decentralized Optimal Control for Large-Scale Multi-agent System by Using Neural Networks and Discrete-time Mean Field Games. In *2021 International Joint Conference on Neural Networks (IJCNN)*, pages 1–6, 2021. doi:10.1109/IJCNN52387.2021.9534288.
- [16] Alex Tong Lin, Samy Wu Fung, Wuchen Li, Levon Nurbekyan, and Stanley J. Osher. Alternating the population and control neural networks to solve high-dimensional stochastic mean-field games. *Proceedings of the National Academy of Sciences*, 118(31):e2024713118, 2021. doi:10.1073/pnas.2024713118.
- [17] René Carmona and Mathieu Laurière. Convergence Analysis of Machine Learning Algorithms for the Numerical Solution of Mean Field Control and Games I: The Ergodic Case. *SIAM Journal on Numerical Analysis*, 59(3):1455–1485, 2021. doi:10.1137/19M1274377.
- [18] René Carmona and Mathieu Laurière. Convergence analysis of machine learning algorithms for the numerical solution of mean field control and games: II—the finite horizon case. *The Annals of Applied Probability*, 32, 12 2022. doi:10.1214/21-AAP1715.
- [19] Mouhcine Assouli and Badr Missaoui. Deep Policy Iteration for high-dimensional mean field games. *Applied Mathematics and Computation*, 481:128923, 2024. ISSN 0096-3003. doi:10.1016/j.amc.2024.128923.
- [20] Mouhcine Assouli and Badr Missaoui. Deep learning for Mean Field Games with non-separable Hamiltonians. *Chaos, Solitons & Fractals*, 174:113802, 2023. ISSN 0960-0779. doi:10.1016/j.chaos.2023.113802.
- [21] Noufel Frikha, Maximilien Germain, Mathieu Laurière, Huyên Pham, and Xuanye Song. Actor-Critic learning for mean-field control in continuous time. *arXiv*, 03 2023. doi:10.48550/arXiv.2303.06993.
- [22] Zejian Zhou and M. Sami Fadali and Hao Xu. Biomimetic Optimal Tracking Control using Mean Field Games and Spiking Neural Networks. *IFAC-PapersOnLine*, 53(2):8112–8117, 2020. ISSN 2405-8963. doi:10.1016/j.ifacol.2020.12.2281. 21st IFAC World Congress.
- [23] Sriram Ganapathi Subramanian, Matthew E. Taylor, Mark Crowley, and Pascal Poupart. Partially Observable Mean Field Reinforcement Learning. In *Proceedings of the 20th International Conference on Autonomous Agents and MultiAgent Systems*, page 537–545, 2021. doi:10.48550/arXiv.2012.15791.
- [24] Timothy Lillicrap, Jonathan Hunt, Alexander Pritzel, Nicolas Heess, Tom Erez, Yuval Tassa, David Silver, and Daan Wierstra. Continuous Control with Deep Reinforcement Learning. *CoRR*, 09 2015. doi:10.48550/arXiv.1509.02971.
- [25] Sarah Perrin, Mathieu Laurière, Pérolat Julien, Matthieu Geist, Romuald Elie, and Olivier Pietquin. Mean Field Games Flock! The Reinforcement Learning Way. In *Proceedings of the Thirtieth International Joint Conference on Artificial Intelligence (IJCAI-21)*, pages 356–362, 08 2021. doi:10.24963/ijcai.2021/50.
- [26] Berkay Anahtarci, Can Deha Kariksiz, and Naci Saldi. Q-Learning in Regularized Mean-field Games. *Dynamic Games and Applications*, 13(1):89–117, 2023. doi:10.1007/s13235-022-00450-2.
- [27] Rajesh Mishra, Deepanshu Vasal, and Sriram Vishwanath. Model-Free Reinforcement Learning for Mean Field Games. *IEEE Transactions on Control of Network Systems*, 10(4):2141–2151, 2023. doi:10.1109/TCNS.2023.3264934.

- [28] Ricky T. Q. Chen, Yulia Rubanova, Jesse Bettencourt, and David K. Duvenaud. Neural ordinary differential equations. *Advances in Neural Information Processing Systems*, 31, 2018. doi:10.48550/arXiv.1806.07366.
- [29] J. Su and J. E. Renaud. Automatic Differentiation in Robust Optimization. *AIAA Journal*, 35 (6):1072–1079, June 1997. doi:10.2514/2.196.
- [30] Hans Peters. *Game Theory: A Multi-Leveled Approach*. Springer, 2008. ISBN 978-3-540-69290-4. p. 169.
- [31] René Carmona, François Delarue, et al. *Probabilistic Theory of Mean Field Games with Applications I-II*. Springer Nature, 3 2018. ISBN 978-3-319-56437-1.
- [32] Robert A. Adams and Christopher Essex. *Calculus: A Complete Course*. Pearson, Ontario, 8 edition, 2013. ISBN 978-0-32-178107-9.
- [33] Kaiming He, Xiangyu Zhang, Shaoqing Ren, and Jian Sun. Deep Residual Learning for Image Recognition. In *2016 IEEE Conference on Computer Vision and Pattern Recognition (CVPR)*, pages 770–778, 2016. doi:10.1109/CVPR.2016.90.
- [34] L.S. Pontryagin, E.F. Mishchenko, G.V. Boltyanskii, and R.V. Gamkrelidze. *Mathematical Theory of Optimal Processes*. Interscience Publishers, 1962. ISBN 9782881240775.
- [35] Christopher Rackauckas, Yingbo Ma, Julius Martensen, Collin Warner, Kirill Zubov, Rohit Supekar, Dominic Skinner, Ali Ramadhan, and Alan Edelman. Universal differential equations for scientific machine learning. *arXiv preprint arXiv:2001.04385*, 2020. doi:10.48550/arXiv.2001.04385.
- [36] Juntang Zhuang, Tommy Tang, Yifan Ding, Sekhar Tatikonda, Nicha Dvornek, Xenophon Papademetris, and James S. Duncan. AdaBelief Optimizer: Adapting Stepsizes by the Belief in Observed Gradients. In *Proceedings of the 34th International Conference on Neural Information Processing Systems, NIPS '20*, Red Hook, NY, USA, 2020. Curran Associates Inc. ISBN 9781713829546.
- [37] Patrick Kidger. *On Neural Differential Equations*. PhD thesis, University of Oxford, 2021.
- [38] Patrick Kidger and Cristian Garcia. Equinox: neural networks in JAX via callable PyTrees and filtered transformations. *Differentiable Programming workshop at Neural Information Processing Systems 2021*, 2021.
- [39] Igor Babuschkin, Kate Baumli, Alison Bell, Surya Bhupatiraju, Jake Bruce, Peter Buchlovsky, David Budden, Trevor Cai, Aidan Clark, Ivo Danihelka, Antoine Dedieu, Claudio Fantacci, Jonathan Godwin, Chris Jones, Ross Hemsley, Tom Hennigan, Matteo Hessel, Shaobo Hou, Steven Kapturovski, Thomas Keck, Iurii Kemaev, Michael King, Markus Kunesch, Lena Martens, Hamza Merzic, Vladimir Mikulik, Tamara Norman, George Papamakarios, John Quan, Roman Ring, Francisco Ruiz, Alvaro Sanchez, Laurent Sartran, Rosalia Schneider, Eren Sezener, Stephen Spencer, Srivatsan Srinivasan, Miloš Stanojević, Wojciech Stokowiec, Luyu Wang, Guangyao Zhou, and Fabio Viola. The DeepMind JAX Ecosystem, 2020. URL <http://github.com/deepmind>.
- [40] Brian W. Arthur. Inductive Reasoning and Bounded Rationality. *The American Economic Review*, 84(2):406–411, 1994. URL <https://www.jstor.org/stable/2117868>.
- [41] Robert J. Aumann and Lloyd S. Shapley. *Values of non-atomic games*. Princeton University Press, 2015. doi:10.1515/9781400867080.
- [42] Noam Brown. Equilibrium Finding for Large Adversarial Imperfect-Information Games. *PhD thesis*, 2020.
- [43] David Schmeidler. Equilibrium Points of Non-Atomic Games. *Journal of Statistical Physics*, 7: 295–300, May 1973. doi:10.1007/BF01014905.

A Liar’s logic

The players of the *Liar’s dice* game need to decide at each turn whether they increment or challenge the previous bid. To do so, they follow the logic presented in Algorithm 1.

Algorithm 1 The logic of the individual *Liar’s dice* player i

Global variables: The maximal number of pips on the dice p_{max} , the likelihood threshold $l = 0.3$.

Input: the number of pips p_{t-1} and quantity q_{t-1} of the previous bid b_{t-1} , the player’s dice outcomes d^i , the player’s beliefs about the dice odds $\hat{\theta}_t^i$ and the player’s bluff parameter λ_t^i .

```

 $e \leftarrow \text{estimate\_occurrences}(p_{t-1}, d^i, \hat{\theta}_t^i)$            // Estimate the number of occurrences of  $p_{t-1}$ .
if  $q_{t-1} > e$  then                                       // Increase the number of pips for the new bid.
     $p_t \leftarrow p_{t-1} + 1$ 
    if  $p_t > p_{max}$  then
        return Challenge the previous bid
    end if
else
     $p_t \leftarrow p_{t-1}$ 
end if

if  $\text{bid\_probability}(p_t, q_t, \hat{\theta}_t^i) < l$  then           // Challenge when the new bid seems unlikely.
    return Challenge the previous bid
else
     $q_t \leftarrow q_t + \text{Poisson}(\lambda_t^i)$                  // Add bluff.
    return  $p_t, q_t$                                        // Submit the new bid.
end if

```

B Additional Liar’s dice analyses

B.1 The ratio of successful challenges

As mentioned in Section 4.3.1, a more deceitful playing style of the neural ODE-based players does not seem to increase the ratio of successful challenges. To support this claim, we reproduce Figure 4b and compare it to the ratio of successful challenges presented in Figure 6b. When considering the ratio of successful challenges for $\lambda_0 \leq 6$, the neural ODE-based agents (orange) have a smaller ratio than the purely MFG-based agents (blue). The only exception is found at $\lambda_0 = 0$, where the ratio of successful challenges for the MFG-based agents is very low due to the total absence of bluffing (Figure 6a). However, when $\lambda_0 > 6$, the success ratio of the neural ODE agents is larger than that of the MFG-based agents, even though the strategies of both groups are almost equal (Figure 6a).

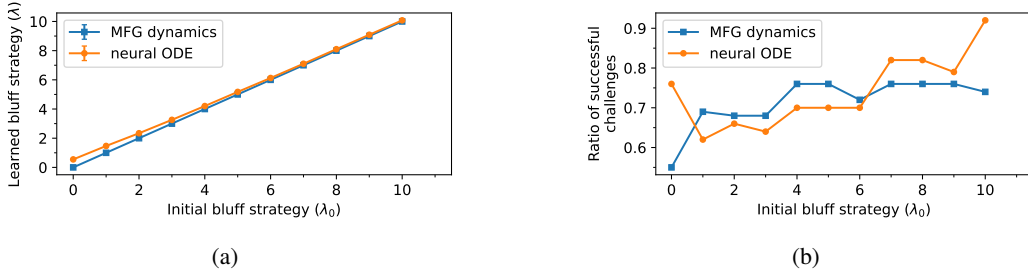


Figure 6: A comparison between the bluffing strategies of the agents that are purely based on the MFG mechanics (blue) and the agents that are based on a neural ODE (orange). All agents have a correct belief about the dice odds. (a) presents the learned versus initial bluff strategy and the ratio of successful challenges as a function of the initial bluff strategy is shown in (b). The results are aggregated over 100 games. The error bars indicate a standard deviation from this average.

B.2 Playing with unfair dice

When analyzing the bluff strategies in the main text and Appendix B.1, we assume that the players' beliefs about the dice are correct. In this section, we do not make this assumption and consider the interaction between the bluff strategy and the players' beliefs about the dice odds. To do so, we again initialize a game with $N = 30$ players having $D = 15$ dice each. However, the players have the uniform initial beliefs that the dice are fair: $\hat{\theta}_t^t = (1/6, 1/6, 1/6, 1/6, 1/6, 1/6)$. In contrast, the actual dice odds are $\theta = (1/10, 2/10, 0/10, 4/10, 1/10, 2/10)$.

The discrepancy between the estimated and true dice odds exaggerates the differences between the bluff strategies of the two groups of players, as shown in Figure 7. Comparing Figure 7a to Figure 4a, the incorrect beliefs of the dice odds mainly seem to influence the game lengths of the MFG-based agents. Yet, the neural ODE-based players tend to bluff more when the players' beliefs are wrong, as presented in Figure 7b. Lastly, the incorrect beliefs have a very strong effect on the ratio of successful challenges of the MFG-based players, converging to 1.0 when $\lambda_0 > 1$ (Figure 7c). While this effect is less strong for the neural ODE-based players, the exact influence of the bluff strategy on the ratio of successful challenges is hard to interpret. Because the dice are unfair, the success of the challenge strongly depends on the probability associated with the number of pips from the bid. The number of pips that are regarded correlates with the game length: the more turns are played, the higher the faces of the considered dice. As a consequence, the results from Figure 7c depend on θ through the game's length and may change if θ changes.

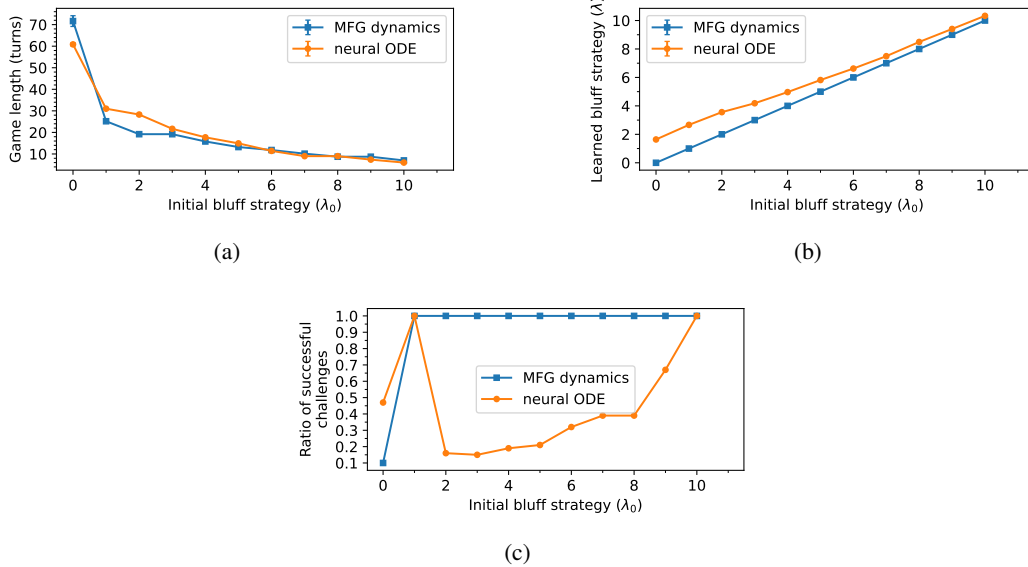


Figure 7: A comparison between bluffing strategies within a game with unfair dice. The strategies of the players that are purely based on the MFG dynamics are shown in blue, and the ones of the neural ODE-based players are shown in orange. (a), the game length as a function of the initial bluff strategy. (b), the learned bluff strategy versus the initial bluff strategy. (c) the relation between the initial bluff strategy and the ratio of successful challenges.